The effects of age on mitochondria, axonal transport, and axonal degeneration after chronic IOP elevation using a murine ocular explant model

Elizabeth C. Kimball[1], **Joan L. Jefferys**[1], **Mary E. Pease**[1], **Ericka N. Oglesby**[1], **Cathy Nguyen**[1], **Julie Schaub**[1], **Ian Pitha**[1,2], and **Harry A. Quigley**[1]

[1]Glaucoma Center of Excellence, Wilmer Eye Institute, Johns Hopkins University, Baltimore, MD, USA

[2]The Center for Nanomedicine, Wilmer Eye Institute, Johns Hopkins University, Baltimore, MD, USA

Abstract

The purpose of this study was to compare younger and older mice after chronic intraocular pressure (IOP) elevation lasting up to 4 days with respect to mitochondrial density, structure, and movement, as well as axonal integrity, in an *ex vivo* explant model. We studied 2 transgenic mouse strains, both on a C57BL/6J background, one expressing yellow fluorescent protein (YFP) in selected axons and one expressing cyan fluorescent protein (CFP) in all mitochondria. Mice of 4 months or 14 months of age were exposed to chronic IOP by anterior chamber microbead injection for 14 hours, 1, 3, or 4 days. The optic nerve head of globe--optic nerve explants were examined by laser scanning microscopy. Mitochondrial density, structure, and movement were quantified in the CFP explants, and axonal integrity was quantified in YFP explants. In control mice, there was a trend towards decreased mitochondrial density (# per mm2) with age when comparing younger to older, control mice, but this was not significant ($1,947 \pm 653$ vs $1,412 \pm 356$; $p = 0.19$). Mitochondrial density decreased after IOP elevation, significantly, by 31%, in younger mice ($p = 0.04$) but trending towards a decrease, by 22%, in older mice ($p=0.82$) compared to age matched controls. Mitochondrial mean size was not altered after chronic IOP elevation for 14 hours or more (p 0.16). When assessing mitochondrial movement, in younger mice, 5% were mobile at any given time; 4% in the anterograde direction and 1% retrograde. In younger untreated tissue, only 75% of explants had moving mitochondria (mean = 15.8 moving/explant), while after glaucoma induction only 24% of explants had moving mitochondria (mean = 4.2 moving/explant; difference from control, $p = 0.03$). The distance mitochondria traveled in younger mice was unchanged after glaucoma exposure, but in older glaucoma explants the distance traveled was less than half of older controls ($p < 0.0003$). In younger mice, mitochondrial speed increased after 14 hours of elevated IOP ($p = 0.006$); however, in older glaucoma explants, movement was actually slower

Corresponding Author: Elizabeth C. Kimball, Smith Building M002, Wilmer Eye Institute, Johns Hopkins University, 400 North Broadway, Baltimore, MD USA 21287; telephone: +1 410 955 3337; fax: +1 443 287 2711; fcone1@jhmi.edu.

than controls (p = 0.02). In RGC-YFP explants, axonal integrity declined significantly after 4 days of IOP elevation to a similar degree in both younger and older mice. Older mice underwent greater loss of mitochondrial movement with chronic IOP elevation than younger mice, but suffered similar short-term axonal fragmentation in C57BL/6J mice. These transgenic strains, studied in explants, permit observations of alterations in intracellular structure and organelle activity in experimental glaucoma.

Keywords

Glaucoma; sclera; mouse; retinal ganglion cell; axons; mitochondria; transport block; explant

1.0 Introduction

Glaucoma is the most common preventable cause of blindness worldwide (Quigley and Broman, 2006). Elevated intraocular pressure (IOP, Anderson and Hendrickson 1974, Quigley et al., 1981) causes vision impairment by death of retinal ganglion cells (RGC) and remodeling of the optic nerve head (ONH). Older age (Burgoyne and Downs, 2007) and myopia (Boland and Quigley, 2007) are known risk factors for open angle glaucoma. Glaucoma animal models been used to further our understanding of RGC loss in glaucoma. This includes mouse lines that have been genetically modified to have fluorescent astrocytes (Nguyen et al., 2017), axons (Johnson et al., 2016, Kalesnykas et al., 2012, Li et al., 1999, Leung et al., 2011), and mitochondria (Kang et al., 2008, Miller and Sheetz, 2004, Shen and Cai, 2012). These tools permit assessment of initial effects after chronic IOP exposure. We developed (Kimball et al., 2017) an *ex vivo* explant of the eye and optic nerve to study acute and chronic effects of IOP elevation in mice. In the present research, we studied explants from the two mouse strains, one with yellow fluorescent protein (YFP) in a select number of RGC and a second strain with cyan fluorescent protein (CFP) in all mitochondria. The explant model permits the study of living RGC and mitochondria in their natural environment, though without an active blood supply. By comparison to research with cultured RGC (Welsbie et al., 2013), retinal explants (Johnson et al., 2016, Bull et al., 2011) or eye cup (Ishikawa et al., 2014, Howell et al., 2007, El-Danaf et al., 2015), the axons of our model system are in their original configuration at the ONH. Tissues imaged in this manner are subject to the biomechanical effects of IOP, which can be controlled during observations by maintaining set levels.

IOP elevation alters RGC axonal transport in both the anterograde and retrograde directions, in human (Quigley and Green, 1979), monkey (Gaasterland and Kupfer 1974) and rodent (Morrison et al., 1990) eyes. RGC are provided with energy from adenosine triphosphate, often distributed by mitochondria that travel along the axon or from mitochondria in neighboring astrocytes (Morrison et al., 2013). While it is known that the movement of mitochondria and other organelles along the axon is interrupted at the level of the sclera within the ONH, the precise mechanism(s) that are disturbed are not yet fully elucidated. In addition, the differences in resistance to glaucoma injury by age of the subject (Boland and Quigley, 2007, Chrysostomou et al., 2010) among different strains of experimental mice has

been demonstrated (Cone et al., 2010, Myers et al., 2010, Steinhart et al., 2013). The reasons for greater damage in some older animals have not yet been determined.

In a pilot study using the ONH explants, we studied the effects of 1–3 hours of acute IOP elevation, along with 4 explants that had undergone prior IOP elevation for 3 days. In the present report, we extensively studied the changes in mitochondrial structure, density and movement, as well as axonal integrity, in explants that had undergone prior IOP elevation for up to 4 days. We compared quantitative alterations in 4 month old mice and 14–17 month old mice of the C57BL/6J strain on which the two transgenics are based.

2.0 Methods

2.1. Animals

Animals were treated in accordance with the ARVO Statement for the Use of Animals in Ophthalmic and Vision Research, using protocols approved and monitored by the Johns Hopkins Animal Care and Use Committee. In this study, two transgenic mouse strains were used, one expressing YFP in selected axons (B6.Cg-Tg(Thy-1YFP)HJrs/J, Jackson Catalog Number 3782, RGC-YFP) and a second expressing CFP in all mitochondria (B6.Cg-Tg(Thy-1CFP/COX8A)S2Lich/J, Jackson Catalog Number 7967, Mito-CFP). Both types of mice were bred in a C57BL/6J background, obtained from Jackson Laboratories (Bar Harbor, ME), and expressed YFP or CFP under the control of the mouse thymus cell antigen 1, theta (Thy1) promoter. In YFP mice, the fluorescent marker was expressed in only a small proportion of RGCs. In CFP mice, all mitochondria of many cell types were fluorescent, due to linkage to human cytochrome c oxidase, subunit 8A (ubiquitous), targeting signal fused to the N-terminus. We studied a total of 41 animals, 16 RGC-YFP and 26 Mito-CFP mice, with 31 and 47 explants respectively, as both eyes of most animals were utilized (Table 1). Twenty-nine explants were from 4 month old mice of the Mito-CFP strain, 18 explants were from 14 month old Mito-CFP mice, and 31 explants were from 14–17 month old RGC-YFP mice. For comparison to the older RGC-YFP mice, we utilized comparable data on younger (4 months old) mice, published previously (Kimball et al., 2017).

2.2. Chronic IOP Elevation Model

Mice were anesthetized with an intraperitoneal mixture of ketamine (Fort Dodge Animal Health, Fort Dodge, IA), xylazine (VedCo Inc., Saint Joseph, MO) and acepromazine (Phoenix Pharmaceuticals, Burlingame, CA) at 50, 10 and 2 mg/kg concentrations, respectively). To elevate IOP, the anterior chamber of the left eye was injected (Cone et al., 2010) with Polybead Microspheres (Polysciences, Inc., Warrington, PA, USA). The protocol consisted of 2 μL of 6 μm diameter beads, then 2 μL of 1 μm diameter beads, followed by 1 μL of viscoelastic compound (10 mg/ml sodium hyaluronate, Healon; Advanced Medical Optics Inc., Santa Ana, CA). The injections were made through a glass cannula with a 50 μm diameter tip, connected to a Hamilton syringe (Hamilton, Inc., Reno, NV). The contralateral eye (right) was used as a control. Among the bead treated RGC-YFP and Mito-CFP animals, eyes were explanted at one of 3 time points post glaucoma induction; 14 hours, 1 day, or 3–4 days.

2.3. Preparation of Explants

Mice were deeply anesthetized by an intraperitoneal anesthetic injection. IOP measurements were taken with a Tonolab Tonometer (TioLat, Inc., Helsinki, Finland). Each eye, along with a 1.5 mm nerve segment, was enucleated, and the animals were euthanized. A cautery mark on the superior cornea provided subsequent orientation. Eyes were kept in Neurobasal Solution (NB, Thermo Fisher Scientific, Waltham, MA). Axial length and width of the eye were measured using a digital caliper (Instant ReadOut Digital Caliper; Electron Microscopy Sciences, Hatfield, PA, USA). Each globe was glued with cyanoacrylate onto a plastic chuck, superior side facing up. The nerve was placed flat on the chuck surface and 1% agarose (Sigma A4603, St. Louis, MO) that was pre-heated to 37°C was applied to immobilize the optic nerve. Supplemental NB was added after 1 minute to keep the tissue hydrated.

2.4. Imaging of Explants

Imaging was performed on a Zeiss 710 Confocal Laser Scanning Microscope (LSM 710, Carl-Zeiss, Oberkochen, Germany) in two-photon laser (2P) mode (Chameleon Ultra II, Coherent Inc, Santa Clara, CA), using an objective inverter arm with one of two dipping lenses: 20× or 40× W Plan-Apochromat VIS IR series, each with 1.0 NA (Carl-Zeiss, Oberkochen, Germany). Once the eye was securely glued and ON covered in agarose, NB was added and the eye and nerve were positioned underneath the inverter and the 20× lens for RGC-YFP explants and 40× lens for Mito-CFP explants. For the RGC-YFP explants, the 2P laser for LSM imaging was set at 950 nm excitation and the output collected using a 500–550 band pass filter. A series of 2-dimensional full frame images was obtained in 1 μm intervals to a depth of 75–100 μm.

In Mito-CFP explants, the excitation wavelength was 850 nm for mitochondria (pseudo-color blue, and a band-pass filter allowing 500–550 nm for second harmonic generation imaging to demonstrate collagen fibers. The imaging of collagen was performed to identify the position of the ONH. A set of images was obtained as close to the ONH as possible, proximal to the globe, with a time series of 2-dimensional slices at depths up to 60 μm. For measurement of mitochondrial movement, a particular position was reimaged 30 times, every 4 seconds for a total of 2 minutes.

2.5. Axon Integrity

To measure the degree of degeneration in the RGC-YFP explants, the axonal integrity ratio (Knöferle et al., 2010) was used as previously published (Kimball et al., 2017). Each Z-stack of ONH images from RGC-YFP mice was converted into a maximum projection image, allowing all axons from the 70–100 μm thickness to appear within a single 2-dimensional image. Axons that were located within the projection image were marked for subsequent quantification with Zeiss Zen software (Carl-Zeiss, Oberkochen, Germany). The measurement tool was used to measure the total length of each axon. In axons that exhibited gaps with no fluorescence, the length of each fragment (from gap to gap) was measured to derive the number of fragments, the mean fragment length and the total fragment length of all fragments in that axon. The parameter called axon integrity was then calculated by dividing the total length of fragments by the total axon length.

2.6. Mitochondrial Density and Size Quantification

To estimate mitochondrial density and mean individual mitochondrion size, images were converted to an 8-bit, grey scale, 200 μm by 100 μm image window using Photoshop. Using Metamorph Imaging Analysis software, the following parameters were collected: total number of mitochondria per field, minimum diameter (the smallest diameter of each mitochondrion), maximum diameter (the greatest diameter of each mitochondrion), average diameter (average of 20 measurements from center point to exterior edge of each mitochondrion), mitochondrion area (using average diameter calculation), and total area (area of all mitochondria per field). The density of mitochondria was the total number of mitochondria divided by the area of the field of view.

2.7. Mitochondrial Speed and Distance Moved Quantification

Using a specific imaging protocol, we measured mitochondrial speed by acquiring images at the same position every 4 seconds for 2 minutes (30 images total). All moving mitochondria that were visible in successive images were measured using the distance tool of the Zeiss Zen software package. Each mitochondrion was marked in the first image of the time-series in which it was visibly mobile, then it was marked in each image through the stack until it appeared motionless. Nearly all mitochondria movement was in the y-direction (along the axon). Mitochondria that moved in tight circular, repeating patterns were not counted, since they were assumed to be within glial or vascular cells. Speed was calculated by dividing the total distance of movement from the initial to final position by the time elapsed between the images.

2.8 Statistical methods

For the analysis of the density of mitochondria from an explant, all estimates and p-values were generated from generalized linear mixed models (GLMM) with the normal response distribution and the identity link function. Four additional parameters were studied using the same mixed model: total area occupied by mitochondria, the mean mitochondrial diameter, mean maximum diameter, and mean shortest diameter. Analysis of the percent of mitochondria moving in the anterograde and retrograde direction was carried out using GLMM models with binomial response distribution and the logit link function. The outcome variable was number of mitochondria moving in the specified direction divided by the total number of mitochondria observed. All models took into account the correlation in outcome between the two explants of a single mouse by treating mouse as a random effect. Groups in which all explants were taken from different mice were compared using the chi-square test or Student's t-test.

For the analysis of the distance and speed of the mitochondria moving in the anterograde and retrograde direction, all estimates and p-values are from mixed linear models with normal response distribution which take into account the correlation in outcome among the moving mitochondria from a single eye by assuming a compound symmetry covariance structure, in which the correlation in outcome between any two mitochondria from a single explant is the same. The models also take account of the correlation between outcomes from two explants of a single mouse by treating mouse as a random effect. In order for model

residuals to be consistent with a normal distribution, distance in the anterograde direction was transformed by modeling the square root of the natural logarithm of distance.

All estimates and p-values regarding integrity ratio are from one mixed linear model with normal response distribution which takes into account the correlation among the axons from a single eye by assuming a compound symmetry covariance structure, in which the correlation in outcome between any two of these axons is the same. For outcomes for which the groups to be compared were composed of explants from different mice, the chi-square test or Student's t-test were used.

For all analyses, the Bonferroni method was used to adjust significance levels for multiple comparisons from a single model. All analyses were performed using SAS 9.2 (SAS Institute, Cary, NC).

3.0 Results

3.1. Mitochondrial density decreased with exposure to elevated IOP in both age groups

In control mice, there was a trend towards decreased mitochondrial density (# per mm^2) with age when comparing young to older, control mice, but this was not significant ($1,947 \pm 653$ vs $1,412 \pm 356$; p = 0.19, Table 2). When all glaucoma durations (14 Hour, 1 Day and 3 Day) were grouped together and compared between younger and older mice, exposure to elevated IOP led to a mild trend, but not significant decrease in mitochondrial density (younger glaucoma- $1,361 \pm 549$ vs older glaucoma- $1,111 \pm 429$ respectively, p=0.12). In all younger glaucoma mice (grouped), mitochondrial density decreased significantly by 31% when compared to young controls (p = 0.04, adjusted p-value, Table 2). In older mice, there was a 22% decrease in mitochondria density between older control versus all older glaucoma older animals (p=0.82, adjusted p-value). When analyzing specific time points in young mice, compared to the control tissue, 14 hour and 3 day IOP elevation caused a decrease in mitochondrial density by 39% and 32%, respectively (Figure 1). In older mice, mitochondria density decreased by 22% after 14 hours of glaucoma exposure and 25% after 1 day of glaucoma exposure, but not significantly (p=1.0, and p=1.0 respectively, adjusted p-value).

3.2. Mitochondrial shape and size not significantly changed by age or glaucoma

The typical mitochondrial shape was an elongated oval, with the longer dimension being typically 7 times longer than the narrowest dimension (see Video 1).

When studying mitochondrial size, there was no significant change in diameter after various times of exposure to elevated IOP, in either the younger or the older mice (all adjusted p values 0.60 or greater for differences between individual glaucoma time points and control of same age). The mitochondria mean diameter was greater in younger nerves than in the older control nerves, but not significantly (Table 3). The mean maximum diameter (as measured by twice the longest radius measure) was 4.64 μm for young controls and 4.27 μm for older controls. The younger and older glaucoma groups (all 3-time points together by age) had mean maximum diameters of 4.34 and 3.86 μm, respectively.

3.3. Mitochondrial movement decreased more in older than in younger mice with glaucoma

A total of 47 explants were evaluated for the presence of moving mitochondria. Amongst both ages and three treatment time-point groups studied, 16 explants had 1 mobile mitochondrion. The remaining explants showed no mitochondria moving in the image plane during a 2-minute capture period. In samples with moving mitochondria, we quantified speed, direction and distance traveled.

In 8 younger control explants, 6/8 had a total of 95 moving mitochondria (75% of explants had at least 1 moving mitochondrion, mean = 15.8 moving per explant). On average, in each young control explant video, 5% of mitochondria were moving at any given time. Four percent were moving in the anterograde direction, while 1% were moving in the retrograde direction, a statistically significant difference in movement direction (adjusted p = 0.03, chi-square test, Figure 2).

In younger mice, after glaucoma induction, there was a decrease in moving mitochondria. Among 21 younger glaucoma explants, there was a total of 21 moving mitochondria in 5 explants (24% of explants with any motion, mean = 4.2 moving per explant). Three of the 5 explants with motion were in the shortest glaucoma exposed group (14 hour). The prevalence of moving mitochondria significantly declined with glaucoma exposure in the younger glaucoma mice (p = 0.03, chi square test).

Four of six older explants had a total of 23 moving mitochondria, comprising 67% of explants with any motion, very similar to that of younger controls. However, the mean number of moving mitochondria per explant was 5.8, one-third that of younger controls. Among older glaucoma exposed explants, only 8% (1 of 12) had any moving mitochondria (5 mitochondria in one explant 1 day after IOP elevation; mean = 5.0 moving per explant).

We compared 3 movement parameters between younger and older controls; 1) proportion of mitochondria moving in each direction, 2) their distance moved and 3) the speed of movement. Younger controls had 4.0% moving anterograde, compared to 1.8% moving anterograde in older controls (p = 0.58, adjusted p-value). The proportion of mitochondria moving retrograde was similar in younger and older controls (1.0% vs 1.1%). The distance moved before pausing in younger and older controls was not significantly different. When anterograde movement parameters were compared between the age groups with respect to the effect of chronic IOP elevation, the older glaucoma eyes had less than half the movement distance compared to their controls (p <0.0003, Table 4), while there was no such decrease in younger mice. The distance moved in the retrograde direction was not significantly different between age groups or when comparing control versus glaucoma; however, the number of retrogradely moving mitochondria was relatively small. On average, mitochondria moved similar distances before pausing in both the anterograde and the retrograde directions: 7.89 μm and 7.72 μm, respectively. In nerves of younger animals that were exposed to elevated IOP, mitochondria did not significantly change the distance traveled, in either anterograde or retrograde directions.

In younger control mice, mitochondria moved twice as fast in the retrograde direction compared to the anterograde direction (0.35 μm/s vs. 0.17 μm/s, respectively, p 0.001;

Figure 2). In younger mice, 14 hours of elevated IOP was associated with significantly increased speed in both the anterograde and the retrograde directions.. However, in older mice, almost no mitochondria were moving after 14 hours or 1 day of IOP elevation, and the anterior movement was actually slower than controls (p = 0.01, for anterograde movement).

3.4. Axon integrity ratio decreased with glaucoma exposure regardless of age

In an initial, pilot study describing this method (Kimball et. al., 2017), explants from young RGC-YFP mice were used to measure axonal integrity after acute and chronic pressure elevation. We have included these previously published data from young RGC-YFP to compare to older RGC-YFP mouse explants in the present study (Table 5). In control animals, there was essentially no axonal fragmentation in either younger or older control RGC-YFP explants (mean axon integrity ratio, older control = 0.95, younger control = 1.0; p = 1.00, Figure 3). Fragmentation was significant in eyes exposed to elevated IOP for 14 hours and increased progressively with longer IOP elevation. Axonal integrity ratio declined with time of glaucoma exposure in a linear and statistically significant manner in both younger and older mice (estimated change in integrity ratio/minute (95% CI) = −0.0024 (−0.0038, −0.0010) for younger, −0.0019 (−0.0034, −0.0004) for older mice, p = 0.001 and 0.01, respectively). The regression slope for younger and older mice did not significantly differ (p = 0.61). In younger glaucoma eyes, the integrity ratio was significantly below control values at all 3 time points (Table 5 and Figure 4). In older glaucoma eyes, the decline was somewhat less substantial, but significantly different from older controls at 4 days. The paired differences between younger and older eyes in integrity ratio at each of the 3 time points did not differ significantly (all adjusted p values   0.10).

4.0 Discussion

We used *ex vivo* explants to study the ONH in two transgenic mouse strains for the effect of chronic IOP elevation on mitochondrial behavior and axonal structure. We further compared the response of younger and older mice. The more dramatic effects of IOP elevation were to decrease mitochondrial movement within axons in the ONH. In control explants, we confirmed our previous data that 4–5 times more mitochondria are moving anterograde than retrograde, while the speed of each intermittent movement is greater in the retrograde direction (Kimball et al., 2017). These facts are consistent with studies of mitochondrial motion in cultured neuronal processes (Misgeld et al., 2007). In younger mice, chronic IOP elevation significantly decreased the proportion of axons with mitochondrial movement from 75% to 24% of axons. Similarly, in younger glaucoma explants the number of mitochondria moving per axon fell to one-third of control values with IOP elevation. There were even greater decreases in mitochondrial motion in older mice with IOP elevation. The number of mitochondria moving per axon in control, older RGC was one-third that of younger controls. Furthermore, only 1 of 12 older glaucoma explants had any moving mitochondria at all (compared to 1/4th of younger glaucoma explants). In addition, older glaucoma mice had significantly smaller movement distances compared to their controls, while younger glaucoma mice had no such decrease. Finally, older glaucoma mice had a decrease in anterograde movement speed in the first day after IOP elevation, while younger mice had a transient increases in both anterograde and retrograde speed. Reductions in mitochondrial

movement and speed were detected after laser injury to single, cultured RGC (Yokota et al., 2015).

The function of mitochondria in axons includes the provision of ATP-based energy to drive intra-axonal processes (Bristow et al., 2002). Mitochondria move in axonal transport bidirectionally (Miller and Sheetz, 2006, Kang et al, 2008, Sheng and Cai, 2012), with those moving anterograde (toward the brain) having higher ATP levels than those returning to the cell body (Miller and Sheetz, 2004). Along the axon, mitochondria pause to provide fuel for various pathways. The process of their movement by axonal transport is, itself, energy-dependent. Therefore, their movements could be disturbed by lack of ATP, by reduction in other nutrients (McElnea et al., 2011, Osborne, 2010, and Tezel, 2011) or by constriction of the axon by IOP elevation. Histological studies of experimental glaucoma have documented abnormal accumulations of mitochondria at the ONH (Minckler et al., 1978). Our studies in this explant model have now added dynamic features of the process by which experimental IOP elevation affects mitochondria. We found that fragmented segments of axons begin to appear within the first day after IOP elevation in the mouse and that clumps of mitochondria are found in these swollen areas. The number of individual mitochondria still identifiable as single entities falls somewhat (hence, a fall in density is seen), while many more are included in the clumped zones. As evidence of the detrimental effect of IOP elevation on their transport, there is a substantial decrease both in the proportion of axons with moving mitochondria and in the number of mitochondria moving per axon. Interestingly, of those mitochondria still moving during the first day after IOP elevation, their speed actually increased transiently in young mice. This may be a true increase or it could indicate that the slower moving mitochondria had stopped, leaving only the more rapid ones to be assessed. A final possibility is that the more rapid motion and greater resident time are responses to greater energy need produced by experimental glaucoma. In either case, the abnormalities in mitochondrial motion may be either important causes of axonal dysfunction or responses to the disturbed environment.

Two findings of our previous pilot study of 4 young, chronic glaucoma mice were not confirmed in this detailed study of 33 post-glaucoma explants. The first difference from pilot data was that the density of mitochondria decreased in both younger and older explants with chronic IOP elevation in the present study. There was a modest increase in density in the pilot data. As we have examined more ONH specimens, it has become clear that chronically elevated IOP for up to 4 days leads to swollen axons with clumps of mitochondria bunched together (Kimball et al., 2017). The image analysis system cannot distinguish individual mitochondria in such clumps. Thus, the quantification process would underestimate the true number of mitochondria present—potentially leading to a finding of decreased density. With acute IOP elevation for up to 3 hours, we previously found no change in density. Clearly, the distribution of mitochondria is significantly changed after days of chronic IOP elevation, and in a similar way in both younger and older mouse ONHs. In addition to the much larger number of explants that were studied in the present work, we here concentrated on the ONH within and just behind the posterior sclera, corresponding to the ONH itself. In the previous report, we presented data from this zone, but also from ON zones somewhat further behind the globe.

The second feature in which the present, larger dataset was different from the pilot data was the size of mitochondria. In the 4 pilot glaucoma eyes, mitochondria were significantly smaller after chronic IOP elevation. In the present data, the maximum and mean diameter of mitochondria were not significantly smaller after IOP elevation in either younger or older mice. Fission of mitochondria in response to injury or disease has been reported (Coughlin et al., 2015, Ju et al., 2007, Kim et al, 2015). It is possible that the mitochondria that are clumped within swollen axons may be of a different size, but not counted in these data, since they cannot be individually resolved. After acute IOP elevations for 3 hours, we found significant decrease in mitochondrial size (Kimball et al., 2017), but without changes in density or clumping in that time frame. In summary, the data tend to support the concept that mitochondrial fission may occur as an immediate response to experimental IOP elevation, but may not be a continued feature in ensuing days.

The study of the YFP mice in this explant model provide additional information on early events in axonal degeneration. The axonal integrity ratio showed fragmentation within one day or more of IOP elevation in some RGCs, with gaps developing in the axon, along with swollen areas, similar to that found in the rat optic nerve crush (Koch et al., 2015). The selective expression of YFP in only a few RGCs in this strain permits a view of details such as these that would be impossible to quantify if all axons were fluorescent. Eyes exposed to high IOP develop progressive fragmentation, beginning as early as 14 hours and worsening over the next 3–4 days. Despite differences described above in which older mice had more profound abnormalities in mitochondrial function, older explants showed similar levels of axonal integrity loss to the younger mice, even adjusted for the level of IOP exposure. This is in contrast to the serious loss of mitochondrial movement in older compared to younger mice with experimental IOP elevation. We have previously found (Cone et al., 2010) that the base strain of the mice used here, C57BL/6J, undergo modest loss of RGC in the chronic glaucoma model, and that older mice of this strain are actually less susceptible to RGC loss than younger mice of the same strain. By contrast, CD1 albino mice show greater RGC loss with the same IOP exposure in older mice compared to younger mice. It is challenging to speculate on these age-related aspects of the mitochondrial and axonal integrity data. One possibility is that the mitochondrial findings are not primary drivers of axonal degeneration. More likely, the pathway to axonal integrity loss consists of a number of steps or pathways. Older mice could have more difficulty maintaining mitochondrial transport, but have protective mechanisms that delay axon integrity loss. Many factors, most of them unknown, lead older humans to be more vulnerable to glaucoma. It will be interesting to perform further studies of age-related effects in different strains of mice in order to dissect important pathogenic differences.

The explant model allows study of RGC axonal physiology under conditions in which the eye and first segment of the ON are in their original configurations, including their normal interaction with associated astrocytes. However, some weaknesses of the explant model are shared with retinal explant and cultured RGC studies. The blood supply to the tissue is interrupted and cell physiology is at least disturbed, with time limitations on any study methods. While we have been able to show that cell integrity and mitochondrial movement are intact for some hours in the model (Kimball et al., 2017), it is not possible to consider the tissues as under normal physiological conditions. The YFP strain permits a view of each

axon, but the specific RGCs that are fluorescent may not be typical of the overall optic nerve. Other transgenic strains are now available with selective fluorescence of known RGC types, and these may be worth utilizing in our model system.

In summary, there are clear abnormalities in the density and movement of mitochondrial induced within hours of IOP elevation in a mouse ONH explant model. Mitochondrial movement is more disturbed in older compared to younger mice. Axonal integrity becomes abnormal within the first day of chronic IOP elevation, but no major age difference was detected in axon fragmentation rate.

Supplementary Material

Refer to Web version on PubMed Central for supplementary material.

Acknowledgments

Abbreviations

ONH	Optic Nerve Head
ON	Optic Nerve
IOP	Intraocular pressure
YFP	Yellow Fluorescent Protein
CFP	Cyan Fluorescent Protein
ATP	Adenosine Triphosphate
RGC	Retinal ganglion cells
RGC-YFP	Mouse strain expressing YFP in selected axons
Mito-CFP	Mouse strain expressing CFP in all mitochondria
Thy1	Thymus cell antigen 1, theta promoter
NB	Neurobasal Solution
LSM 710	Zeiss 710 Confocal Laser Scanning Microscope

5.0 References

Anderson DR, Hendrickson A. Effect of intraocular pressure on rapid axoplasmic transport in monkey optic nerve. Invest Ophthalmol. 1974; 13:771–783. [PubMed: 4137635]

Boland MV, Quigley HA. Risk factors and open-angle glaucoma: concepts and applications. J Glaucoma. 2007; 16:406–418. [PubMed: 17571004]

Bristow EA, Griffiths PG, Andrews RM, Johnson MA, Turnbull DM. The distribution of mitochondrial activity in relation to optic nerve structure. Arch Ophthalmol. 2002; 120:791–796. [PubMed: 12049585]

Bull ND, Johnson TV, Welsapar G, DeKorver NW, Tomarev SI, Martin KR. Use of an adult rat retinal explant model for screening of potential retinal ganglion cell neuroprotective therapies. Invest Ophthalmol Vis Sci. 2011; 52:3309–3320. [PubMed: 21345987]

Burgoyne CF, Downs JC. Premise and prediction e how optic nerve head biomechanics underlies the susceptibility and clinical behavior of the aged optic nerve head. J Glaucoma. 2007; 17:318–328.

Chrysostomou V, Trounce IA, Crowston JG. Mechanisms of retinal ganglion cell injury in aging and glaucoma. Ophthalmic Res. 2010; 44:173–178. [PubMed: 20829641]

Cone FE, Gelman SE, Son JL, Pease ME, Quigley HA. Differential susceptibility to experimental glaucoma among 3 mouse strains using bead and viscoelastic injection. Exp Eye Res. 2010; 91:415–424. [PubMed: 20599961]

Coughlin L, Morrison RS, Horner PJ, Inman DM. Mitochondrial morphology differences and mitophagy deficit in murine glaucomatous optic nerve. Invest Ophthalmol Vis Sci. 2015; 56:1437–1446. [PubMed: 25655803]

El-Danaf RN, Huberman AD. Characteristic Patterns of Dendritic Remodeling in Early-Stage Glaucoma: Evidence from Genetically Identified Retinal Ganglion Cell Types. J Neurosci. 2015; 35:2329–2343. [PubMed: 25673829]

Gaasterland D, Kupfer C. Experimental glaucoma in the rhesus monkey. Invest Ophthalmol Vis Sci. 1974; 13:455–457.

Howell GR, Libby RT, Jakobs TC, Smith RS, Phalan FC, Barter JW, Barbay JM, Marchant JK, Mahesh N, Porciattti V, Whitmore AV, Masland RH, John SW. Axons of retinal ganglion cells are insulted in the optic nerve early in DBA/2J glaucoma. J Cell Biol. 2007; 7:1523–1537.

Ishikawa M, Yoshitomi T, Zorumski CF, Izumi Y. Neurosteroids are endogenous neuroprotectants in an ex vivo glaucoma model. Invest Ophthalmol Vis Sci. 2014; 55:8531–8541. [PubMed: 25406290]

Johnson TV, Oglesby EN, Steinhart MR, Cone-Kimball E, Jefferys J, Quigley HA. Time-lapse retinal ganglion cell dendritic field degeneration imaged in organotypic retinal explant culture. Invest Ophthalmol Vis Sci. 2016; 57:253–264. [PubMed: 26811145]

Ju WK, Liu Q, Kim KY, Crowston JG, Lindsey JD, Agarwal N, Ellisman MH, Perkins GA, Weinreb RN. Elevated hydrostatic pressure triggers mitochondrial fission and decreases cellular ATP in differentiated RGC-5 cells. Invest Ophthalmol Vis Sci. 2007; 48:2145–2151. [PubMed: 17460273]

Kalesnykas G, Oglesby EN, Zack DJ, Cone FE, Steinhart MR, Tian J, Pease ME, Quigley HA. Retinal ganglion cell morphology after optic nerve crush and experimental glaucoma. Invest Ophthalmol Vis Sci. 2012; 53:3847–3857. [PubMed: 22589442]

Kang JS, Tian JH, Pan PY, Zald P, Li C, Deng C, Sheng ZH. Docking of axonal mitochondria by syntaphilin controls their mobility and affects short-term facilitation. Cell. 2008; 132:137–148. [PubMed: 18191227]

Kim KY, Perkins GA, Shim MS, Bushong E, Alcasid N, Ju S, Ellisman MH, Weinreb RN, Ju WK. DRP1 inhibition rescues retinal ganglion cells and their axons by preserving mitochondrial integrity in a mouse model of glaucoma. Cell Death Dis. 2015; 6:e1839. [PubMed: 26247724]

Kimball EC, Pease ME, Steinhart MR, Oglesby EN, Pitha I, Nguyen C, Quigley HA. A mouse ocular explant model that enables the study of living optic nerve head events after acute and chronic intraocular pressure elevation: Focusing on retinal ganglion cell axons and mitochondria. Exp Eye Res. 2017; 160:105–115.

Knöferle J, Koch J, Ostendorf J, Michel U, Planchamp V, Vutova P, Tönges L, Stadelmann C, Brück W, Bähr M, Lingora P. Mechanisms of acute axonal degeneration in the optic nerve in vivo. Proc Natl Acad Sci. 2010; 107:6064–6069. [PubMed: 20231460]

Koch JC, Bitow F, Haack J, d'Hedouville Z, Zhang JN, Tönges L, Michel U, Oliveita LM, Jovin TM, Liman J, Tatenhorst L, Bähr M, Lingor P. Alpha-synuclein affects neurite morphology, autophagy, vesicle transport and axonal degeneration in CNS neurons. Cell Death Dis. 2015; 6:1811.

Li Y, Schlamp CL, Nickells RW. Experimental induction of retinal ganglion cell death in adult mice. Invest Ophthalmol Vis Sci. 1999; 40:1004–1008. [PubMed: 10102300]

Leung CK, Weinreb RN, Li ZW, Liu S, Lindsey JD, Choi N, Liu L, Cheung CY, Ye C, Qiu K, Chen LJ, Yung WH, Crowston JG, Pu M, So KF, Pang CP, Lam DS. Long-term in vivo imaging and measurement of dendritic shrinkage of retinal ganglion cells. Invest Ophthalmol Vis Sci. 2011; 52:1539–1547. [PubMed: 21245394]

McElnea EM, Quill B, Docherty NG, Irnaten M, Siah WF, Clark AF, O'Brien CJ, Wallace DM. Oxidative stress, mitochondrial dysfunction and calcium overload in human lamina cribrosa cells from glaucoma donors. Mol Vis. 2011; 17:1182–1191. [PubMed: 21617752]

Miller KE, Sheetz MP. Axonal mitochondrial transport and potential are correlated. J Cell Sci. 2004; 117:2791–2804. [PubMed: 15150321]

Miller KE, Sheetz MP. Direct evidence for coherent low velocity axonal transport of mitochondria. J Cell Biol. 2006; 173:373–381. [PubMed: 16682527]

Minckler DS, Bunt AH, Klock IB. Radiographic and cytochemical ultrastructural studies of axoplasmic transport in the monkey optic nerve head. Invest Ophthalmol Vis Sci. 1978; 17:33–50. [PubMed: 74368]

Misgeld T, Kerschensteiner M, Bareyre FM, Burgess RW, Lichtman JW. Imaging axonal transport of mitochondria in vivo. Nature Methods. 2007; 4:559–561. [PubMed: 17558414]

Morrison JC, Dorman-Pease ME, Dunkelberger GR, Quigley HA. Optic nerve head extracellular matrix in primary optic atrophy and experimental glaucoma. Arch Ophthalmol. 1990; 108:1020–1024. [PubMed: 2369339]

Morrison BM, Lee Y, Rothstein JD. Oligodendroglia: metabolic supporters of axons. Trends Cell Biol. 2013; 12:644–651.

Myers KM, Cone FE, Quigley HA, Gelman S, Pease ME, Nguyen TD. The in vitro inflation response of mouse sclera. Experimental Eye Research. 2010; 91:866–875. [PubMed: 20868685]

Nguyen C, Midgett D, Kimball EC, Steinhart MR, Nguyen TD, Pease ME, Oglesby EN, Jefferys J, Quigley HA. Measuring deformation in the mouse optic nerve head and peripapillary sclera. Invest Opthalmol Vis Sci. 2017; 58:721–733.

Osborne NN. Mitochondria: Their role in ganglion cell death and survival in primary open angle glaucoma. Exp Eye Res. 2010; 90:750–757. [PubMed: 20359479]

Quigley HA, Green WR. The histology of human glaucoma cupping and optic nerve damage: Clinicopathologic correlation in 21 eyes. Ophthalmology. 1979; 10:1803–1827.

Quigley HA, Addicks EM, Green WR, Maumenee AE. Optic nerve damage in human glaucoma. II. The site of injury and susceptibility to damage. Arch Ophthalmol. 1981; 99:635–649. [PubMed: 6164357]

Quigley HA, Broman A. The number of persons with glaucoma worldwide in 2010 and 2020. Br J Ophthalmol. 2006; 90:151–156.

Sheng Z-H, Cai Q. Mitochondrial transport in neurons: impact on synaptic homeostasis and neurodegeneration. Nat Rev Neurosci. 2012; 13:77–93. [PubMed: 22218207]

Steinhart MR, Cone-Kimball E, Nguyen C, Nguyen TD, Pease ME, Chakravarti S, Oglesby EN, Quigley HA. Susceptibility to glaucoma damage related to age and connective tissue mutations in mice. Experimental Eye Research. 2013; 119:54–60. [PubMed: 24368172]

Tezel G. The immune response in glaucoma: a perspective on the roles of oxidative stress. Exp Eye Res. 2011; 93:178–86. [PubMed: 20709058]

Welsbie D, Yang Z, Yan Z, Ge Y, Mitchell KL, Zhou X, Martin SE, Berlinkicke CA, Hackler L Jr, Fuller J, Cao LH, Han B, Auld D, Xue T, Hirai S, Germain L, Simard-Bosson C, Blouin R, Nguyen JV, Davis CH, Enke RA, Boye SL, Merbs SL, Marsh-Armstrong N, Hauswirth WW, DiAntonio A, Nickells RW, Inglese J, Hanes J, Yau KW, Quigley HA, Zack DJ. Functional genomic screening identifies dual leucine zipper kinase as a key mediator of retinal ganglion cell death. Proc Natl Acad Sci. 2013; 110:4045–4050. [PubMed: 23431148]

Yokota S, Takihara Y, Arimura S, Miyake S, Takamura Y, Yoshimura N, Inatani M. Altered transport velocity of axonal mitochondria in retinal ganglion cells after laser-induced axonal injury in vitro. Invest Ophthalmol Vis Sci. 2015; 56:8019–8025. [PubMed: 26720449]

Highlights

- A previously published explant model of the mouse eye was used to facilitate the study of retinal ganglion cell axons and mitochondria in the living optic nerve head, the site of glaucoma injury, of both older and younger mice.

- Using laser scanning microscopy imaging was possible in two transgenic mouse strains; one expressing fluorescent protein in selected retinal ganglion cell axons and another expressing all mitochondria.

- Glaucoma caused fragmentation of axon structures at the ONH, increasing in severity with longer periods of glaucoma exposure. Comparable fragmentation of the RGCs was found between young and older glaucoma exposed mice.

- Glaucoma bead model caused a significant decrease in mitochondria density in both younger and older exposed mice. A significant decrease in mitochondrial movement also occurred after glaucoma bead model exposure in younger and older mice.
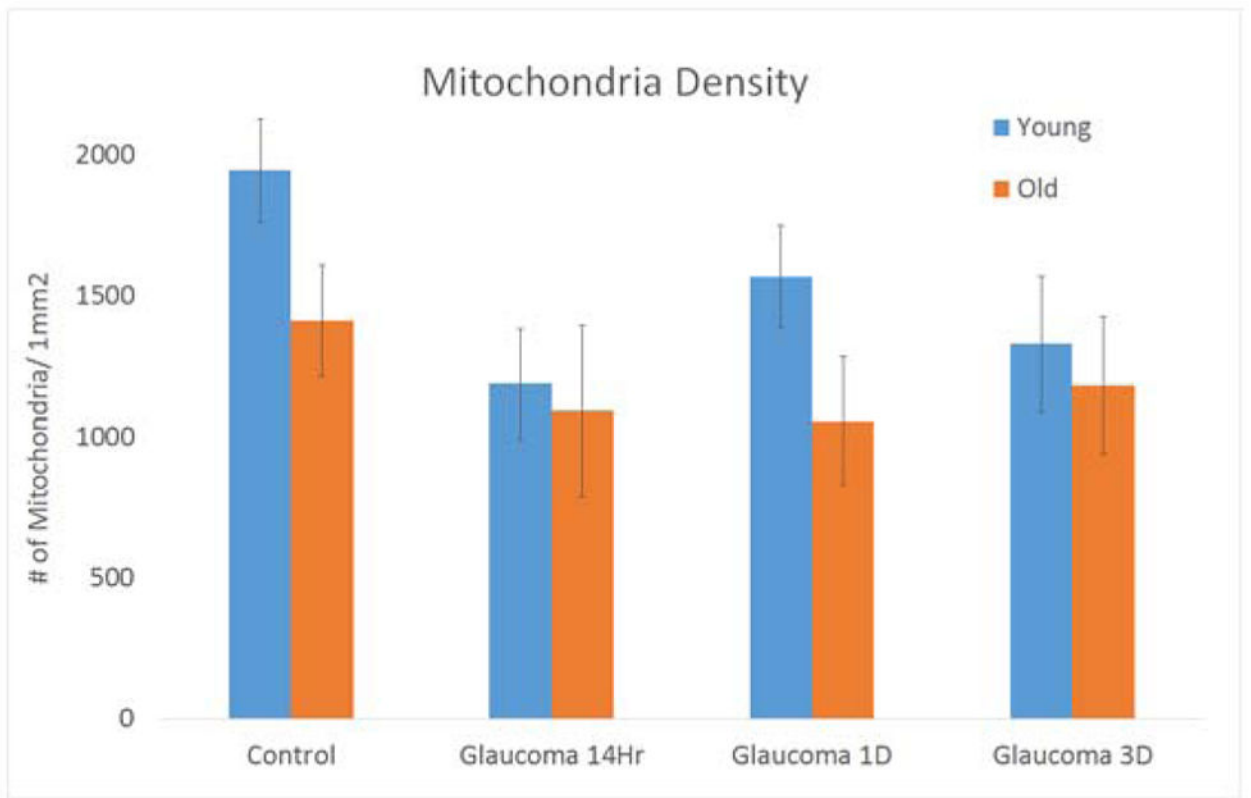
Figure 1.
Mitochondrial density (# of mitochondria in mm2) found in explants of 4 treatments groups; control, glaucoma 14 hours (14 Hr), glaucoma 1 day (1D) and glaucoma 3 days (3D) in both young and old mice. Each graph contains standard error bars
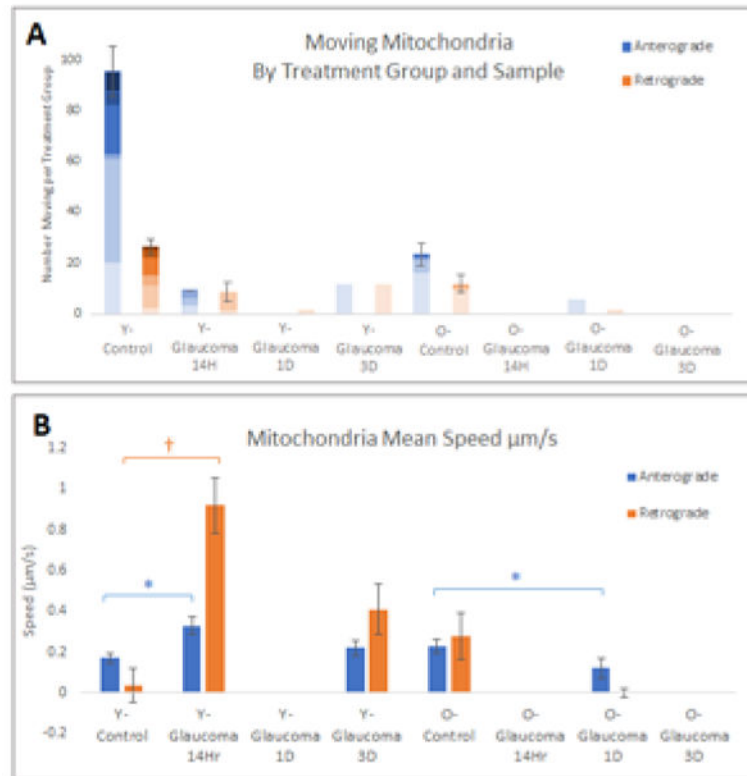
Figure 2.
A) The number of moving mitochondria for each explant sample within each treatment group separated by direction. Each shade represents a single explant. The blue bars represents mitochondria moving in the anterograde direction, the orange bars represent mitochondria moving in the retrograde direction. B) Mitochondrial mean speed by group. The blue bars represents mitochondria moving in the anterograde direction, the orange bars represent mitochondria moving in the retrograde direction. *= p-value is <0.05, †= p value is <0.01 using Bonferroni adjustment for multiple comparisons; (47 Eyes from 26 Mice). Mean values are the speed of mitochondria per 0.2 mm2 (200 µm by 100 µm image window).
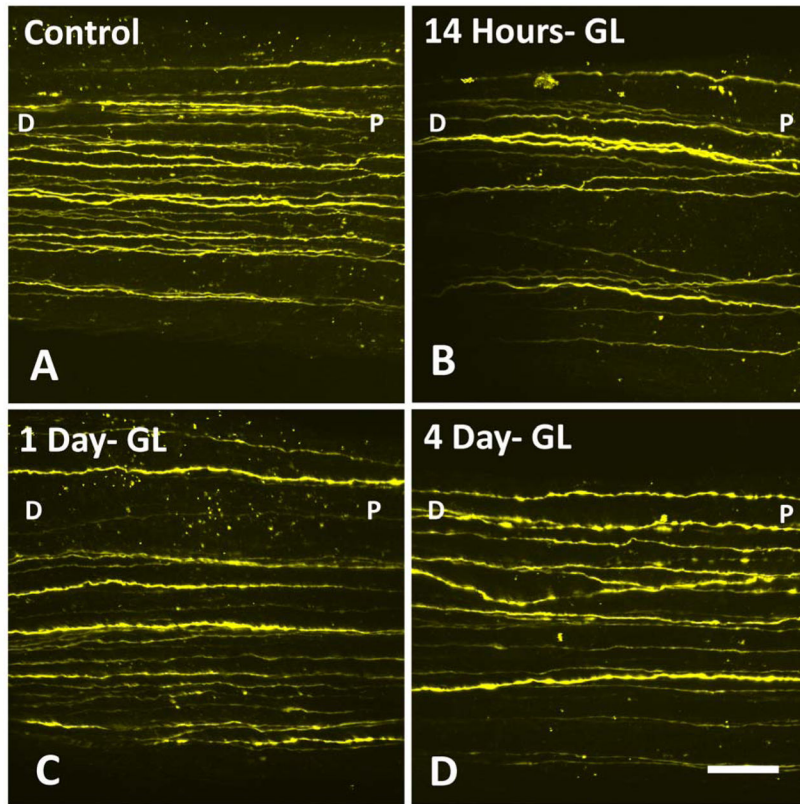
Figure 3.
RGC-YFP axons from older mice show (A) control tissue, and progressive fragmenation, swelling, and loss after IOP elevation in the bead- induced model (B) 14 hours, (C) 1 day, and (D) 4 days post chronic IOP elevation. Labels: D-distal to the eye, P-proximal to the eye (at the ONH) are used to indicate orientation (bar = 30 μm).

Figure 4.
RGC-YFP fluorescent axons of eight different groups were studied to asses fragmentation. Axon integrity was calculated by dividing the total length of fragments by the total axon length. †= p value is <0.01 using Bonferroni adjustment for multiple comparisons

Table 1

Animals in protocols

Strain	Treatment	Age (months)	Experimental Group	N (explants)
Mito-CFP	Control	4	Younger, Control	8
Mito-CFP	14 Hour Glaucoma	4	Younger, Glaucoma 14Hr	8
Mito-CFP	1 Day Glaucoma	4	Younger, Glaucoma 1Day	9
Mito-CFP	3 Day Glaucoma	4	Younger, Glaucoma 3Day	4
Mito-CFP	Control	14	Older, Control	6
Mito-CFP	14 Hour Glaucoma	14	Older, Glaucoma 14Hr	3
Mito-CFP	1 Day Glaucoma	14	Older, Glaucoma 1Day	5
Mito-CFP	3 Day Glaucoma	14	Older, Glaucoma 3Day	4
			Total Mito-CFP	**47**
RGC-YFP	Control	14–17	YFP-Older, Control	18
RGC-YFP	14 Hour Glaucoma	14	YFP-Older, Glaucoma 14Hr	5
RGC-YFP	1 Day Glaucoma	14	YFP-Older, Glaucoma 1Day	5
RGC-YFP	4 Day Glaucoma	14	YFP-Older, Glaucoma 4Day	3
			Total RGC-YFP	**31**

Table 2

Number of mitochondria in control and glaucoma mice

Grouped by Age	Number of Eyes	Mean Density per Image (95% CI)	Pairwise Comparison	Adjusted P-value[*]
Young, Control (Y-C)	8	1947 (1561, 2334)	Y-C, O-C	0.26
Young, Glaucoma (Y-G)	21	1361 (1109, 1614)	Y-C, Y-G	**0.04**
Old, Control (O-C)	6	1412 (994, 1830)		
Old, Glaucoma (O-G)	8	1111 (792, 1430)	O-C, O-G	0.82

[*] Bonferroni adjustment for multiple comparisons; (47 Eyes from 26 Mice). Mean estimated values are the number of mitochondria per 1.0 mm^2 (Calculated by multiplying the 200 μm by 100 μm image window, 0.2 mm^2 by 5 to).

Table 3

Mitochondrial diameter

Group	Mean Mitochondrial Diameter, μm (95% CI)	Pairwise Comparison	Adjusted P-value[*]
Young, Control (Y-C)	2.52 (2.31, 2.74)	Y-C, O-C	0.68
Young, Glaucoma (Y-G)	2.40 (2.27, 2.54)	Y-C, Y-G	0.92
Old, Control (O-C)	2.34 (2.11, 2.57)		
Old, Glaucoma (O-G)	2.18(2.00, 2.36)	O-C, O-G	0.66

[*] data from 47 Eyes from 26 Mice

Table 4

Anterograde movement distance

Group	Mean Distance, μm (95% CI)	Pairwise Comparison	Adjusted P-value*
Young, Control (Y-C)	7.89 (5.73, 11.15)	Y-C, O-C	1.00
Young, Glaucoma (Y-G)	8.19 (5.46, 12.81)	Y-C, Y-G	1.00
Old, Control (O-C)	10.33 (6.67, 16.74)		
Old, Glaucoma (O-G)	4.08 (2.64, 6.81)	O-C, O-G	**< 0.0003**

Data from 16 eyes of 12 mice.

Author Manuscript   Author Manuscript   Author Manuscript   Author Manuscript

Table 5

Axon integrity with glaucoma exposure

Group	# Nerves	# Axons	# Fragments per Axon	Median Fragment Length	Mean Total Fragment Length	Mean Axon Length
Young, Control	3	23	1.0	353	388 ± 38	393 ± 38
Young, 14 hr GL	6	77	8.0	35	318 ± 108	395 ± 55
Young, 1 day GL	5	29	6.0	34	341 ± 147	375 ± 81
Young, 4 day GL	7	34	6.5	21	215 ± 139	379 ± 91
Old, Control	18	294	3.0	420	368 ± 92	383 ± 78
Old, 14 hr GL	5	76	9.5	40	345 ± 109	395 ± 64
Old, 1 day GL	5	46	9.0	26	268 ± 115	307 ±113
Old, 4 day GL	3	44	11.0	25	288 ±97	393 ± 50

GL = glaucoma group; hr = hour

*
The data for younger RGC-YFP mice is from explants whose data were reported previously (Kimball et al., 2017).